

Device-independent quantum secret sharing with advanced random key generation basis

Qi Zhang¹, Jia-Wei Ying², Zhong-Jian Wang¹, Wei Zhong³, Ming-Ming Du², Shu-Ting Shen²,
Xi-Yun Li¹, An-Lei Zhang¹, Shi-Pu Gu², Xing-Fu Wang¹, Lan Zhou^{1*}, Yu-Bo Sheng²

¹*College of Science, Nanjing University of Posts and Telecommunications,
Nanjing, Jiangsu 210023, China*

²*College of Electronic and Optical Engineering and College of Flexible Electronics (Future Technology),
Nanjing University of Posts and Telecommunications,
Nanjing, Jiangsu 210023, China*

³*Institute of Quantum Information and Technology,
Nanjing University of Posts and Telecommunications,
Nanjing, Jiangsu 210003, China*

(Dated: October 8, 2024)

Quantum secret sharing (QSS) enables a dealer to securely distribute keys to multiple players. Device-independent (DI) QSS can resist all possible attacks from practical imperfect devices and provide QSS the highest level of security in theory. However, DI QSS requires high-performance devices, especially for low-noise channels, which is a big challenge for its experimental demonstration. We propose a DI QSS protocol with the advanced random key generation basis strategy, which combines the random key generation basis with the noise preprocessing and postselection strategies. We develop the methods to simplify Eve's conditional entropy bound and numerically simulate the key generation rate in an acceptable time. Our DI QSS protocol has some advantages. First, it can increase the noise tolerance threshold from initial 7.147% to 9.231% (29.16% growth), and reduce the global detection efficiency threshold from 96.32% to 93.41%. The maximal distance between any two users increases to 1.43 km, which is about 5.5 times of the initial value. Second, by randomly selecting two basis combinations to generate the key, our DI QSS protocol can reduce the entanglement resource consumption. Our protocol has potential for DI QSS's experimental demonstration and application in the future.

I. INTRODUCTION

Quantum communication aims to guarantee the unconditional communication security based on the fundamental principles of quantum mechanics. As a multipartite cryptographic primitive [1–3], quantum secret sharing (QSS) is one of the main quantum communication branches. QSS divides the key of the dealer into multiple parts and distributes each part to a player. Any subset of players cannot reconstruct the distributed key, which can only be reconstructed when all the players cooperate [1].

The first QSS protocol based on the Greenberger-Horne-Zeilinger (GHZ) state was proposed in 1999 [1]. Since then, QSS has been widely studied both in theory and experiment [2–24]. Like other quantum communication branches, such as quantum key distribution (QKD), the practical imperfect experimental devices may cause serious security loopholes [25–27]. The device-independent (DI) paradigm provides a promising method to guarantee the security based on the nonlocal correlation of the measurement results [28]. DI type protocols can defend against all possible attacks from practical experimental devices and provide the highest level of secu-

rity [29–33]. The research of DI-type protocols started in the DI QKD system [31–33]. Since 2020, DI theory have been introduced into the quantum secure direct communication field [34–36]. In 2022, DI QKD's experiments have achieved significant breakthroughs [37–39], thus proving the feasibility of the DI theory. The research on DI QSS has been started since 2019. Refs. [40, 41] proved DI QSS's correctness and completeness under a causal independence assumption regarding measurement devices. In 2024, the DI QSS protocol based on the violation of Svetlichny inequality was proposed [42]. This protocol first characterized DI QSS's performance in a practical noisy communication scenario by numerically simulating its key generation rate, global detection efficiency threshold, noise threshold, and the maximal communication distance between any two users. Similar as DI QKD protocols [32, 33], DI QSS protocol requires quite high global detection efficiency and has low noise resistance [42]. In particular, as DI QSS requires to distribute multi-photon entanglement to multiple users while DI QKD only requires to distribute EPR state to two users, DI QSS is more vulnerable to channel loss and limited detection efficiency. It requires ultra-low-noise settings with the global detection efficiency as high as 96.32% and the noise threshold of 7.148% [42].

In the DI QKD field, some active improvement strategies have been put forward to enhance its noise resistance and reduce the high detection efficiency requirement, including noise preprocessing [43–45], postselection [44–

*Email address: zhou@njupt.edu.cn

47], random key generation basis [46, 48], and advantage distillation [49]. For example, the adoption of the noise preprocessing strategy increase DI QKD's noise threshold from initial 7.1492% to 8.0848% [44, 46]. By combining the random postselection and noise preprocessing strategies, DI QKD's global detection efficiency threshold was further reduced to less than 87.49%. Benefit for the improvement strategies, the first DI QKD experiment in the optical platform is experimentally demonstrated [39]. In 2021, the DI QKD protocol with random key generation basis strategy was proposed [48], which effectively improved the noise tolerance threshold from the initial 7.15% to 8.24%. However, the estimation of Eve's conditional entropy bound is quite complicated, which requires about 5000 core hours and thus largely increases the difficulty of parameter optimization. Soon later, Ref. [46] simplified the DI conditional entropy bound and provided the optimal entropy in a much shorter time (less than one second). It largely reduced the difficulty of parameter optimization and further improved DI QKD's noise tolerance threshold to 8.36%. The noise preprocessing combined with the random random postselection strategy was also introduced into the DI QSS protocol [42], which can reduce its global detection efficiency threshold from 96.32% to 94.30% and increase the noise threshold from 7.148% to 8.072%.

Although the above improvement can reduce DI QSS's experimental difficulty, the experimental demonstration of DI QSS is still a big challenge. Meanwhile, the DI QSS protocol [42] only uses one basis combination to generate the key and discards the measurement results for the other basis combination, which is a waste of precious entanglement resources. For further enhancing DI QSS's noise resistance, and reducing the global detection efficiency and the entanglement resource consumption, we propose the DI QSS protocol with advanced random key generation basis strategies, which combine the random key generation basis, noise preprocessing, and postselection strategies. We develop the technique in Ref. [46] to simplify Eve's conditional entropy bound and numerically simulate its performance in the practical noise environment. The advanced random key generation basis strategy can increase DI QSS's noise tolerance threshold from 7.147% to 9.231% (29.16% growth) and reduce the global detection efficiency requirement from initial 96.32% to 93.41% ($q \rightarrow 0.5$). In this way, the maximal secure communication distance between any two users can be increased from 0.26 km to 1.43 km (about 5.5 times). Based on the above features, our DI QSS protocol with advanced random key generation basis strategy can effectively facilitate DI QSS's experimental implementations and application in the future quantum communication field.

The paper is organized as follows. In Sec. II, we briefly describe the tripartite joint key generation process and the detection of genuine tripartite nonlocal correlations. In Sec. III, we present the DI QSS protocol with the random key generation basis. In Sec. IV, we reduce the

conditional entropy bound problem of the two-basis variant to qubit system to estimate its key generation rate in the practical noisy channel environment. In Sec. V, we combine the noise preprocessing strategy to further enhance DI QSS's resistance to channel noise. Finally, we make some discussion and draw a conclusion in Sec. VI.

II. TRIPARTITE JOINT KEY GENERATION AND GENUINE TRIPARTITE NONLOCAL CORRELATION DETECTION

In the DI QSS, three users' devices are successively repeated for n ($n \rightarrow \infty$) rounds. Their measurement results have two purposes: (1) some rounds of measurement results are used to generate the joint key bits and estimate the qubit error rate (QBER); (2) some rounds of measurement results are used to estimate the genuine tripartite nonlocal correlation among three users' results for security checking.

A. Tripartite joint key generation with the random key generation basis strategy

In this subsection, we explain the joint key generation rules of our DI QSS protocol with the random key generation basis strategy. Suppose that three users Alice, Bob and Charlie share a three-photon GHZ state with the form of

$$|GHZ\rangle = \frac{1}{\sqrt{2}} (|HHH\rangle + |VVV\rangle), \quad (1)$$

where $|H\rangle$ and $|V\rangle$ denote the horizontal and vertical polarization of the photon, respectively.

Three users independently and randomly perform measurement on each photon in their own locations with the bases A_i , B_j , and C_k , respectively, where $i, k \in \{1, 2\}$ and $j \in \{1, 2, 3\}$. In detail, Alice has two measurement bases $A_1 = \sigma_x$, $A_2 = \sigma_y$, Bob has three measurement bases $B_1 = \sigma_x$, $B_2 = \frac{\sigma_x - \sigma_y}{\sqrt{2}}$, $B_3 = \frac{\sigma_x + \sigma_y}{\sqrt{2}}$, and Charlie has two measurement bases $C_1 = \sigma_x$, $C_2 = -\sigma_y$, where σ_x and σ_y are Pauli operators with the eigenstates as

$$\begin{aligned} |+_x\rangle &= \frac{1}{\sqrt{2}} (|H\rangle + |V\rangle), | -_x\rangle = \frac{1}{\sqrt{2}} (|H\rangle - |V\rangle), \\ |+_y\rangle &= \frac{1}{\sqrt{2}} (|H\rangle + i|V\rangle), | -_y\rangle = \frac{1}{\sqrt{2}} (|H\rangle - i|V\rangle). \end{aligned} \quad (2)$$

Their binary measurement results are denoted as $a_i, b_j, c_k \in \{-1, +1\}$, respectively, where $|+_x\rangle$ and $|+_y\rangle$ are labeled as $+1$, while $| -_x\rangle$ and $| -_y\rangle$ are labeled as -1 .

Two measurement basis combinations $\{A_1 B_1 C_1\}$ and $\{A_2 B_1 C_2\}$ are used for the joint key generation. The key generation includes two cases.

Measurement information	Alice			
	$ +\rangle_a$	$ -\rangle_a$	$ +\rangle_a$	$ -\rangle_a$
$ +\rangle_b$	$ +\rangle_c$	$ -\rangle_c$	$ +\rangle_c$	$ -\rangle_c$
$ -\rangle_b$	$ -\rangle_c$	$ +\rangle_c$	$ -\rangle_c$	$ +\rangle_c$
Bob	Charlie			

TABLE I: (Color online) Relationships of three users' measurement results. Alice's measurement results are shown in the first row, and Bob's measurement results are shown in the first column. Charlie's measurement results appear in the boxes.

Case 1: The users measure the three photons in a GHZ state with the basis combination $\{A_1B_1C_1\}$. They can obtain

$$|GHZ\rangle = \frac{1}{2} \left(|+\rangle_a |+\rangle_b |+\rangle_c + |+\rangle_a |-\rangle_b |-\rangle_c + |-\rangle_a |+\rangle_b |-\rangle_c + |-\rangle_a |-\rangle_b |+\rangle_c \right). \quad (3)$$

Case 2: The users measure three photons with the basis combination $\{A_2B_1C_2\}$, where

$$|GHZ\rangle = \frac{1}{2} \left(|+\rangle_a |+\rangle_b |+\rangle_c + |+\rangle_a |-\rangle_b |-\rangle_c + |-\rangle_a |+\rangle_b |-\rangle_c + |-\rangle_a |-\rangle_b |+\rangle_c \right). \quad (4)$$

In above cases, the relationship among the users' measurement results is summarized in Tab. I. If Charlie knows Alice's and Bob's measurement bases, he can know whether Alice's and Bob's measurement results are identical or opposite, but he cannot explicitly know Alice's and Bob's specific measurement results.

We label the measurement result +1 as the key bit 0, and -1 as 1. The relationship among the measurement results in Tab. I can be summarized as $K_A = K_B \oplus K_C$, where K_A , K_B , and K_C denote the key bits of Alice, Bob, and Charlie, respectively.

B. Genuine tripartite nonlocal correlation detection

The genuine tripartite nonlocality can be detected by the Bell-type inequality for three-qubit systems, called the Svetlichny inequality [50]. With the above measurement bases in Sec. II A, the Svetlichny polynomial S_{ABC} can be written as

$$S_{ABC} = \langle a_1 b_2 c_2 \rangle + \langle a_1 b_3 c_1 \rangle + \langle a_2 b_2 c_1 \rangle - \langle a_2 b_3 c_2 \rangle + \langle a_2 b_3 c_1 \rangle + \langle a_2 b_2 c_2 \rangle + \langle a_1 b_3 c_2 \rangle - \langle a_1 b_2 c_1 \rangle. \quad (5)$$

Here, $\langle a_i b_j c_k \rangle$ is the expected value of the tripartite measurement results with the form of $\langle a_i b_j c_k \rangle = P(a_i b_j c_k = 1) - P(a_i b_j c_k = -1)$

(P represents the probability). If the three photons are in classical correlation, S_{ABC} satisfies the Svetlichny inequality $S_{ABC} \leq 4$. The violation of Svetlichny inequality ($S_{ABC} > 4$) implies the existence of the genuine tripartite nonlocality.

For the three-photon GHZ state, S_{ABC} can be simplified by the CHSH polynomials as [51]

$$S_{ABC} = \langle S_{ABC_2} \rangle + \langle S'_{AB_1C_1} \rangle. \quad (6)$$

Here, S_{AB} and S'_{AB} are the general CHSH polynomial and its equivalent variation between Alice's and Bob's measurement results with the form of

$$S_{AB} = \langle a_1 b_2 \rangle + \langle a_2 b_2 \rangle + \langle a_1 b_3 \rangle - \langle a_2 b_3 \rangle, \\ S'_{AB} = \langle a_2 b_3 \rangle + \langle a_2 b_2 \rangle + \langle a_1 b_3 \rangle - \langle a_1 b_2 \rangle, \quad (7)$$

with $\langle a_i b_j \rangle = P(a_i b_j = 1) - P(a_i b_j = -1)$.

For simplicity, we define S to represent S_{AB} or S'_{AB} based on the following rule

$$S = \begin{cases} S'_{AB}, & \text{if } c_1 = +1, \\ -S'_{AB}, & \text{if } c_1 = -1, \\ S_{AB}, & \text{if } c_2 = +1, \\ -S_{AB}, & \text{if } c_2 = -1. \end{cases} \quad (8)$$

With the definition, the violation of Svetlichny inequality equals to Alice's and Bob's measurement results violating the CHSH inequality ($S > 2$) [51].

III. DI QSS PROTOCOL WITH RANDOM KEY GENERATION BASIS STRATEGY

Here, we explain our DI QSS protocol with random key generation basis strategy. Similar to previous DI protocols [31–36, 52–54], the security of this DI QSS protocol can be guaranteed by two basic assumptions, say, the quantum physics is correct and all users' physical locations are secure. Meanwhile, the three users must be legitimate and honest. Three users' devices are repeatedly used for n ($n \rightarrow \infty$) rounds. The schematic diagram of DI QSS protocol with random key generation basis strategy is shown in Fig. 1, which includes the following five steps:

Step 1 Entanglement distribution. The central entanglement source prepares n pairs of three-photon polarization GHZ states (1). The source divides the three photons in each GHZ state into E_1 , E_2 , and E_3 sequences. All the photons in the three sequences are sequentially transmitted to Alice, Bob, and Charlie, respectively.

Step 2 Measurement basis selection. Three users independently and randomly select the measurement bases to measure all photons in the sequences E_1 , E_2 , and E_3 , respectively. The measurement bases A_i , B_j , and C_k are described in Sec. II A, where $i, k \in \{1, 2\}$ and $j \in \{1, 2, 3\}$. The tripartite measurement results are denoted as a_i , b_j , and c_k , where $a_i, b_j, c_k \in \{-1, +1\}$. The

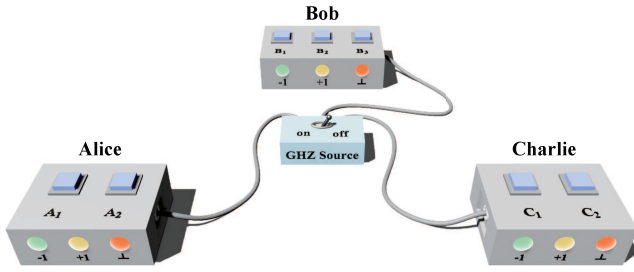


FIG. 1: (Color online) Schematic diagram of the DI QSS protocol with random key generation basis strategy. The central entanglement source prepares n identical three-photon GHZ states, which are split into three sequences, namely E_1 , E_2 , and E_3 sequences. The photons in three sequences are distributed to three remote users, Alice, Bob, and Charlie, respectively. The three users independently select the measurement settings (i , j and k) and record the measurement results: -1 , $+1$, or no-click event \perp .

detector's no-click event \perp is randomly noted as -1 or $+1$, which is called the postselection operation.

Step 3 Parameter estimation. After all measurements, Alice, Bob, and Charlie sequentially announce the measurement basis for each photon. According to the measurement basis selection, the parameter estimation can be categorized into three cases.

Case 1: Bob chooses the measurement basis B_2 or B_3 . In this case, all three users announce the measurement results, which are used to estimate the Svetlichny polynomial S_{ABC} and the CHSH polynomial S . When $2 < S \leq 2\sqrt{2}$ (equivalent to $4 < S_{ABC} \leq 4\sqrt{2}$), the corresponding results at three users' locations have genuine nonlocal correlation. The user can bound the key leakage rate to Eve, thus the photon transmission process is secure and the communication continues. When $S \leq 2$ (equivalent to $S_{ABC} \leq 4$), the measurement results are only classical correlated. The users cannot detect Eve's attacking. In this way, the users regard that the photon transmission process is not secure, and the communication should be terminated.

Case 2: When the measurement basis combination is $\{A_1B_1C_1\}$ or $\{A_2B_1C_2\}$. Alice randomly announces a part of her measurement results, and Bob (Charlie) announces his corresponding measurement results to estimate the QBER δ . The users preserve the remaining unannounced measurement results as the raw key bits.

Case 3: When the measurement basis combination is $\{A_1B_1C_2\}$ or $\{A_2B_1C_1\}$, the users have to discard their measurement results.

Step 4 Error correction and private amplification. The users repeat the above process until all the users have obtained a sufficient number of secure key bits. Then, the users perform the error correction and private amplification on the raw key bits, eventually forming a series of secure key bits.

Step 5 Secret reconstruction. Charlie announces his key bit K_C , and Bob combines his key bit K_B to

reconstruct the key bit K_A delivered by Alice based on the encoding rule in Sec. II A.

IV. THE PERFORMANCE EVALUATION OF THE DI QSS PROTOCOL WITH RANDOM KEY GENERATION BASIS STRATEGY

In this section, we evaluate the performance of the DI QSS protocol with random key generation basis strategy in the practical noisy environment against collective attacks. We assume that Alice (Charlie) uses measurement basis A_1 (C_1) and A_2 (C_2) with probabilities p and $\bar{p} = 1 - p$, respectively.

The users generate the raw key bits when the measurement basis combination is $\{A_1B_1C_1\}$ or $\{A_2B_1C_2\}$. In the asymptotic limit of a large number of rounds, we calculate the asymptotic key generation rate r_∞ , which is the ratio of the extractable key length to measurement rounds n ($n \rightarrow \infty$). Taking into account the ‘‘sifting’’ effect, the asymptotic key generation rate can be written as [46, 48]

$$r_\infty = p^2 r_{111} + \bar{p}^2 r_{212} = (p^2 + \bar{p}^2) (\lambda r_{111} + \bar{\lambda} r_{212}), \quad (9)$$

where $\lambda = p^2/(p^2 + \bar{p}^2)$ represents the matching weight for two key generation basis combinations, and $\bar{\lambda} = 1 - \lambda$. We adopt the Devetak-Winter bound [55, 56] to estimate the key generation rates corresponding to the measurement basis combination $\{A_1B_1C_1\}$ and $\{A_2B_1C_2\}$. The Devetak-Winter bound is a universal method for calculating the key rate in the quantum cryptography field, which has been widely used in QKD and QSS systems [57–60], and extended to DI QKD and one-side DI QSS systems under the collective attack assumption [43, 49, 61–63]. In the asymptotic limit of a large number of rounds, the key generation rates corresponding to the measurement basis combination $\{A_1B_1C_1\}$ and $\{A_2B_1C_2\}$ can be provided by [42, 55, 56]

$$\begin{aligned} r_{111} &= H(A_1|E) - H(A_1|B_1, C_1), \\ r_{212} &= H(A_2|E) - H(A_2|B_1, C_2), \end{aligned} \quad (10)$$

where $H(|)$ is the conditional von Neumann entropy. $H(A_1|E)$ and $H(A_2|E)$ estimate the uncertainty of Eve's knowledge about Alice's key bits when he knows Charlie's key bits, say, the key secrecy rate to Eve corresponding to the measurement basis combinations $\{A_1B_1C_1\}$ and $\{A_2B_1C_2\}$, respectively. $H(A_1|B_1, C_1)$ and $H(A_2|B_1, C_2)$ quantify the tripartite raw key irrelevance with the measurement basis combinations $\{A_1B_1C_1\}$ and $\{A_2B_1C_2\}$, respectively. Therefore, Eq. (9) is rewritten as

$$\begin{aligned} r_\infty &= (p^2 + \bar{p}^2) \left[(\lambda H(A_1|E) + \bar{\lambda} H(A_2|E)) \right. \\ &\quad \left. - (\lambda H(A_1|B_1, C_1) + \bar{\lambda} H(A_2|B_1, C_2)) \right]. \end{aligned} \quad (11)$$

A. The total key secrecy rate to Eve

We apply the similar parameter estimation technique in [46] in our DI QSS protocol with random key generation basis strategy. Firstly, we consider the total key secrecy rate to Eve, which is the first term in Eq. (11). We define the total key secrecy rate to Eve as $H(A|E)$ with the form of

$$H(A|E) = \lambda H(A_1|E) + \bar{\lambda} H(A_2|E). \quad (12)$$

Under the collective attack model [32, 33, 42], the key secrecy rate to Eve is a function of CHSH polynomial S between Alice and Bob. A rough lower bounds on $H(A_1|E)$ and $H(A_2|E)$ are given by

$$H(A_1|E) = H(A_2|E) \geq 1 - \phi \left(\sqrt{\frac{S^2}{4} - 1} \right), \quad (13)$$

where $\phi(x) = h(\frac{1}{2} + \frac{1}{2}x)$ and the binary Shannon entropy $h(x) = -x \log_2 x - (1-x) \log_2 (1-x)$. We define the lower bound function $g(x) = 1 - \phi(x)$, which is a convex function.

In the DI scenario, we consider that all devices are untrusted. In this way, the measurement basis used by three users is potentially under Eve's control, so all measurement bases need to be reparametrized in the following analysis, as described in Appendix A. We use the qubit uncertainty relation to maximally bound the conditional entropy of Alice's key generation. In this way, $H(A|E)$ is bounded by

$$\begin{aligned} H(A|E) &= \lambda H(A_1|E) + \bar{\lambda} H(A_2|E) \\ &\geq g \left(\sqrt{\lambda \langle \bar{A}_1 \otimes B \rangle^2 + \bar{\lambda} \langle \bar{A}_2 \otimes B' \rangle^2} \right). \end{aligned} \quad (14)$$

Here, the Pauli observations \bar{A}_1 and \bar{A}_2 are orthogonal to A_1 and A_2 in the X-Y plane of the Bloch sphere, respectively. B and B' are observations with any given eigenvalue ± 1 on Bob's subsystem. In DI-type protocols, we cannot directly obtain the correlation between Alice's and Bob's subsystems $\langle \bar{A}_i \otimes B \rangle$. Inspired by Ref. [46], Eve's information about the measurement results corresponding to A_1 and A_2 bases can be maximized by the correlation operator of Bob's subsystem with the virtual complementary \bar{A}_1 and \bar{A}_2 .

Based on the correlations among Alice, Bob, and Charlie, *i.e.*, the CHSH polynomial S (Svetlichny polynomial S_{ABC}), we establish a DI qubit correlation bound on $\langle \bar{A}_i \otimes B \rangle$. This process is explained in detail in Appendix

A, which requires to solve the maximization problem as

$$\begin{aligned} E_\lambda(S)^2 &= \max_{s,t} \quad s^2 g^2 + c^2 h^2 + 2(2\lambda - 1)scgh\Delta, \\ &\quad s.t. \quad cg + sh \geq S/2, \\ &\quad \quad \quad g^2 \leq 1, \\ &\quad \quad \quad h^2 \leq 1, \\ &\quad \quad \quad (1-g^2)(1-h^2) \geq g^2 h^2 \Delta^2, \\ &\quad \quad \quad c^2 + s^2 = 1, \\ &\quad \quad \quad \Delta^2 \leq 1, \end{aligned} \quad (15)$$

where we parameterize the Pauli operator correlation $\langle \sigma_x \otimes \sigma_x \rangle = g \cos \gamma$, $\langle \sigma_x \otimes \sigma_y \rangle = g \sin \gamma$, $\langle \sigma_y \otimes \sigma_x \rangle = h \cos \mu$, $\langle \sigma_y \otimes \sigma_y \rangle = h \sin \mu$, $\Delta = \cos(\gamma - \mu)$. We obtain the virtual orthogonal operator $\bar{A}_i = (-1)^{i-1} \sin \frac{\varphi_A}{2} \sigma_x + \cos \frac{\varphi_A}{2} \sigma_y$ and $s = \sin \frac{\varphi_A}{2}$, $c = \cos \frac{\varphi_A}{2}$.

Then, the conditional entropy bound of Eq. (14) is given by

$$H(A|E) \geq g \left(\tilde{E}_\lambda(S) \right), \quad (16)$$

where $\tilde{E}_\lambda(S) \equiv \sqrt{\tilde{E}_\lambda(S)^2}$, and $\tilde{E}_\lambda(S)^2$ is the maximum value that can be obtained by numerically and analytically solving the optimization problem (15). Finally, a convexity analysis of the DI entropy bound is performed [46].

In Fig. 2, we use CHSH polynomial S between Alice's and Bob's measurement results to quantify $H(A|E)$. For example, with $S = 2.4$, when Alice (Charlie) equally ($p = 50\%$) uses A_1 or A_2 (C_1 or C_2) to measure the photon, $H(A|E) = 0.467$ can be obtained. It is higher than the value of 0.346 corresponding to Alice (Charlie) only using A_1 (C_1) to generate the key ($p = 100\%$). Higher $H(A|E)$ enables our DI QSS protocol with random key generation basis strategy to have stronger noise resistance.

B. The key generation rate in practical noise model

During practical long-distance photon transmission, photon loss and decoherence caused by the channel noise are unavoidable, which can severely degrade the entanglement and weaken the nonlocal correlation among users' measurement results. Here, we consider the common white noise model, which has been widely adopted in DI QKD protocols [33, 43–47]. In the white noise model, the target GHZ state may degenerate to eight possible GHZ states with equal probability. Meanwhile, we assume that each user successfully detects the transmitted photon with the probability of η , and the no-click event occurs with the probability of $\bar{\eta} = 1 - \eta$. In this way, after distributing the entangled photons, three users share

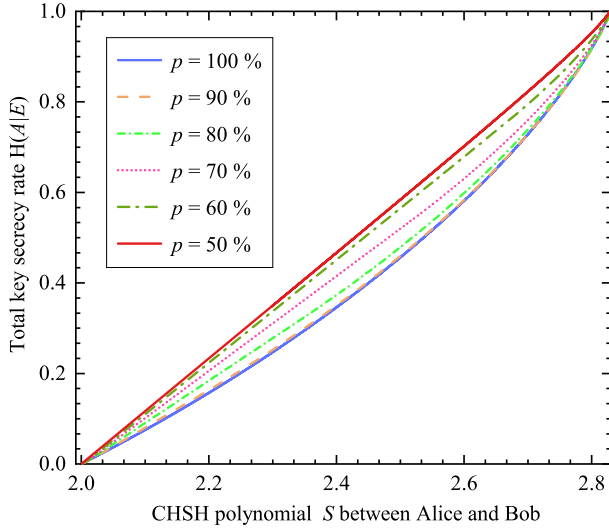


FIG. 2: (Color online) The total key secrecy rate to Eve $H(A|E)$ as a function of the CHSH polynomial S between Alice's and Bob's photons. Here, we fix the probability that Alice (Charlie) chooses measure A_1 (C_1) as $p = 100\%$, 90% , 80% , 70% , 60% , 50% , respectively. The calculation results corresponding to $p = 0, 10\%, 20\%, 30\%, 40\%$ are consistent with those corresponding to $p = 100\%, 90\%, 80\%, 70\%, 60\%$, respectively.

n pairs of identical mixed states with the form of

$$\begin{aligned}
\rho'_{ABC} &= \eta^3 \rho_{ABC} + (1-\eta)^3 |vac\rangle\langle vac| \\
&+ \frac{1}{2} \eta^2 (1-\eta) (|HH\rangle\langle HH| + |VV\rangle\langle VV|)_{BC} \\
&+ \frac{1}{2} \eta^2 (1-\eta) (|HH\rangle\langle HH| + |VV\rangle\langle VV|)_{AC} \\
&+ \frac{1}{2} \eta^2 (1-\eta) (|HH\rangle\langle HH| + |VV\rangle\langle VV|)_{AB} \\
&+ \frac{1}{2} \eta (1-\eta)^2 (|H\rangle\langle H| + |V\rangle\langle V|)_A \\
&+ \frac{1}{2} \eta (1-\eta)^2 (|H\rangle\langle H| + |V\rangle\langle V|)_B \\
&+ \frac{1}{2} \eta (1-\eta)^2 (|H\rangle\langle H| + |V\rangle\langle V|)_C, \quad (17)
\end{aligned}$$

where $|vac\rangle$ denotes the vacuum state, and

$$\rho_{ABC} = F |GHZ\rangle\langle GHZ| + \frac{1-F}{8} I. \quad (18)$$

The fidelity F is the probability that no error occurs in the photonic state, and the unit matrix I is composed by the density matrices of the eight possible noisy GHZ states.

We first consider the case that all photons in the GHZ states are successfully detected by three users. According to the coding rule $K_A = K_B \oplus K_C$, four GHZ states will make three users obtain incorrect measurement results corresponding to the key generation basis combinations $\{A_1 B_1 C_1\}$ and $\{A_2 B_1 C_2\}$ (see Appendix B). Therefore,

the QBER Q_1 caused by the white noise model is

$$Q_1 = Q_{111} = Q_{212} = \frac{1}{2} (1-F). \quad (19)$$

Then, we analyze the influence from the photon loss. In addition to the successful detection results $+1$ ($|+_x\rangle$ and $|+_y\rangle$) and -1 ($|-_x\rangle$ and $|-_y\rangle$), each user randomly defines the no-click event as an output $+1$ or -1 . The violation of Bell-type inequalities can still be observed only if the photon loss is sufficiently weak (*i.e.*, the global detection efficiency is sufficiently high). The QBER Q_2 caused by the photon loss is

$$\begin{aligned}
Q_2 &= \frac{3}{2} \eta^2 (1-\eta) + \frac{3}{2} \eta (1-\eta)^2 + \frac{1}{2} (1-\eta)^3 \\
&= \frac{1}{2} (1-\eta^3). \quad (20)
\end{aligned}$$

Thus, combining the decoherence and photon loss factors, the total QBER δ after transmitting photons through the noisy channel is

$$\begin{aligned}
\delta &= Q_1 + Q_2 = \frac{1-F}{2} \eta^3 + \frac{1}{2} (1-\eta^3) \\
&= \frac{1}{2} - \frac{1}{2} \eta^3 F. \quad (21)
\end{aligned}$$

In this way, the raw key irrelevance for the three users $H(A_1|B_1, C_1)$ and $H(A_2|B_1, C_2)$ have the form of

$$\begin{aligned}
H(A_1|B_1, C_1) &= h(Q_{111}) = h(\delta), \\
H(A_2|B_1, C_2) &= h(Q_{212}) = h(\delta), \quad (22)
\end{aligned}$$

and the asymptotic key generation rate r_∞ in Eq. (11) can be calculated as

$$r_\infty = (p^2 + \bar{p}^2) [\lambda H(A_1|E) + \bar{\lambda} H(A_2|E) - h(\delta)]. \quad (23)$$

Based on above calculations, the theoretical value of the CHSH polynomial S between Alice's and Bob's measurement results is

$$S = 2\sqrt{2} F \eta^3 = 2\sqrt{2} (1-2\delta). \quad (24)$$

By substituting Eq. (16) and Eq. (24) into Eq. (23), the lower bound of DI QSS's key generation rate r_∞ is given by

$$r_\infty \geq (p^2 + \bar{p}^2) \left[g \left(\tilde{E}_\lambda \left(2\sqrt{2} (1-2\delta) \right) \right) - h(\delta) \right]. \quad (25)$$

Fig. 3 demonstrates the key generation rate r_∞ when Alice (Charlie) chooses A_1 (C_1) to generate the key with the probability $p = 100\%$, 90% , 80% , 70% , 60% , 50% , respectively. The case that Alice (Charlie) only uses A_1 (C_1) ($p = 100\%$) to generate the raw key [42] has the noise tolerance threshold of 7.147%. With the reduction of p , the noise tolerance threshold of the DI QSS protocol can be effectively increased, for Eve's uncertainty about the key generation basis is increased. The maximal

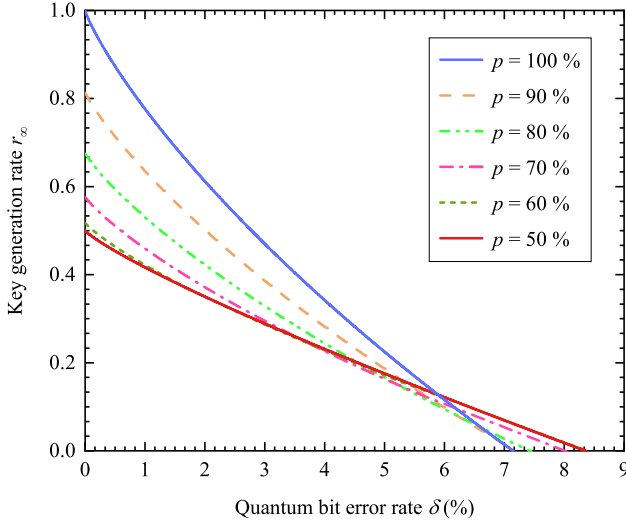


FIG. 3: (Color online) The key generation rate r_∞ as a function of QBER. Alice (Charlie) chose A_1 (C_1) to measure the key generation rate with probabilities $p = 100\%$, 90% , 80% , 70% , 60% , 50% , respectively.

noise tolerance threshold of 8.358% can be achieved under the random key generation basis strategy ($p = 50\%$). Such gain leads to a slight reduction in the maximal key generation rate due to the rise of the probability of measurement basis combination mismatch ($2p(1-p)$). For example, with $\delta = 3\%$, the adoption of the random key generation basis strategy ($p = 50\%$) reduces DI QSS's key generation rates from 0.470 to 0.289. The reduction effect reduces with the growth of noise error rate. When $\delta = 5\%$, the adoption of the random key generation basis strategy reduces the key generation rate from 0.225 to 0.176.

V. THE DI QSS PROTOCOL WITH ADVANCED RANDOM KEY GENERATION BASIS STRATEGY

For further increasing the noise tolerance threshold of our DI QSS protocol, we adopt the noise preprocessing strategy in our DI QSS protocol. Noise preprocessing is an important active improvement strategy, which can effectively increase the noise tolerance threshold of DI QKD [43, 46, 47] and DI QSS protocols [42]. Here, we combine the noise preprocessing with the random key generation basis strategies, which is called the advanced random key generation basis strategy.

The DI QSS protocol only requires minor changes as follows. When the measurement basis combination is $\{A_1B_1C_1\}$ or $\{A_2B_1C_2\}$, Alice flips her measurement result ($+1 \rightarrow -1$, $-1 \rightarrow +1$) with the probability of q . This operation essentially introduces some artificial noise to Alice's measurement results, which can further decrease the correlation among three users' measurement results, and increase Eve's uncertainty about the key bits. As

a result, the net effect on the key generation rate can be positive. After all the measurements, Alice will announce the flip probability q in the error correction process. Then, three users apply a hash function to the raw key bits to get the final secure key bits.

With the advanced random key generation basis strategy, the total noise qubit error rate (NQBER) δ_q consists of two components. First, the initial measurement results do not suffer from bit-flip errors but are flipped by Alice with the probability of q . Second, the initial measurement results suffer from bit-flip error and are not flipped by Alice with the probability of $\bar{q} = 1 - q$. Therefore, δ_q is given by

$$\delta_q = q(1 - \delta) + (1 - q)\delta = q + (1 - 2q)\delta. \quad (26)$$

In this way, the tripartite raw key irrelevance becomes

$$H(A_1|B_1, C_1)_q = H(A_2|B_1, C_2)_q = h(\delta_q). \quad (27)$$

According to the derivation of the DI QSS protocol with noise preprocessing strategy [42], after the noise preprocessing, the lower bound of the total key secrecy to Eve is

$$\begin{aligned} H(A^q|E) &= \lambda H(A_1^q|E) + \bar{\lambda} H(A_2^q|E) \\ &\geq g\left(\sqrt{\lambda \langle \bar{A}_1 \otimes B \rangle^2 + \bar{\lambda} \langle \bar{A}_2 \otimes B' \rangle^2}, q\right), \end{aligned} \quad (28)$$

where

$$g(x, q) = 1 + \phi\left(\sqrt{(1 - 2q)^2 + 4q(1 - q)x^2}\right) - \phi(x). \quad (29)$$

The right part of Eq. (28) has the same bound of that in Eq. (14) [46] (see Appendix A).

Finally, by substituting Eq. (24), Eq. (26)-Eq. (28) into Eq. (11), we can obtain a lower bound of the key generation rate r_∞^q of DI QSS with the advanced random key generation basis strategy as

$$\begin{aligned} r_\infty^q &\geq (p^2 + \bar{p}^2) \left[g\left(\tilde{E}_\lambda\left(2\sqrt{2}(1 - 2\delta)\right), q\right) \right. \\ &\quad \left. - h(q + (1 - 2q)\delta) \right]. \end{aligned} \quad (30)$$

When $q = 0$, Eq. (30) degenerates into Eq. (25).

In Fig. 4, the noise tolerance thresholds of the DI QSS protocol with one key generation basis ($p = 100\%$, dashed lines) and two random key generation basis ($p = 50\%$, solid lines) both increase with the growth of the flipping probability q . When using the same level (same color) of artificial noise (same value of q), the noise tolerance thresholds of the DI QSS protocol with the advanced random key generation basis strategy ($p = 50\%$, solid lines) are all higher than that only uses one key generation basis ($p = 100\%$, dashed lines). In detail, the advanced random key generation basis strategy ($q = 40\%$ and $p = 50\%$) can improve the noise tolerance of the DI

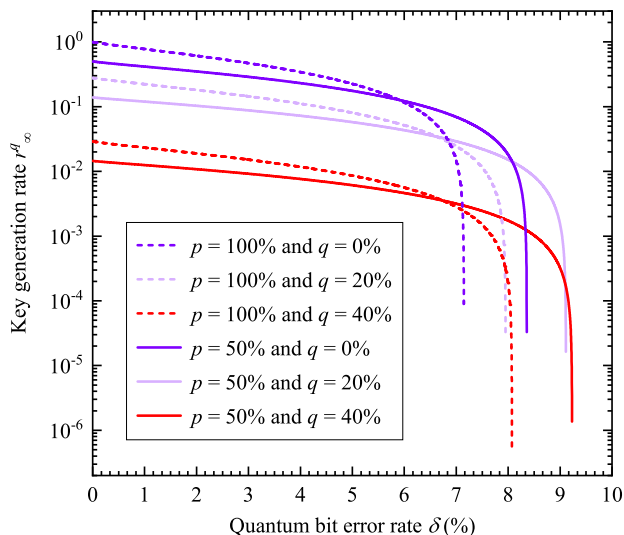


FIG. 4: (Color online) The key generation rate r_∞^q as a function of the QBER δ_q with different values of p and q . The maximal noise tolerance threshold is further improved by using the noise preprocessing strategy ($q = 20\%$, 40%).

QSS protocol from 7.148% (blue dashed line) to 9.231% (red solid line) (29.16% growth).

We define the global detection efficiency $\eta = \eta_t \eta_d \eta_c$, where η_d is the detection efficiency of the photon detector and η_c is the coupling efficiency of the photon to the fiber. The photon transmission efficiency in noisy quantum channel is $\eta_t = 10^{-\frac{\alpha L}{10}}$, where L denotes the photon transmission distance, $\alpha = 0.2$ dB/km for the standard optical fiber. In theory, the growth of noise tolerance threshold would effectively reduce the global detection efficiency threshold. Then, we calculate the global detection efficiency threshold of the DI QSS protocol with the fidelity $F = 1$. From Fig. 5, the adoption of the advanced random key generation basis strategy ($q = 40\%$) can reduce the global detection efficiency threshold from initial 96.32% to 93.42%, which is further lower than 94.30% corresponding to the adoption of the advanced postselection strategy (combining noise preprocessing with $q = 40\%$ and the postselection strategies) [42]. As a result, the advanced random key generation basis strategy can effectively reduce the requirement on experimental equipment's performance and facilitate DI QSS's experimental realization.

Fig. 6 simulates the key generation rate of the DI QSS protocol in five scenarios altered with the photon transmission distance L . The five scenarios include the DI QSS without any active improve strategy, with noise preprocessing strategy ($q = 20\%$), with postselection strategy, with advanced post selection strategy (combining noise preprocessing and post selection strategies), and advanced random key generation basis strategy. Recently, the superconducting nanowire single-photon detector (SNSPD) with a detection efficiency of 98% at 1550 nm band was reported [64]. Therefore, we assume

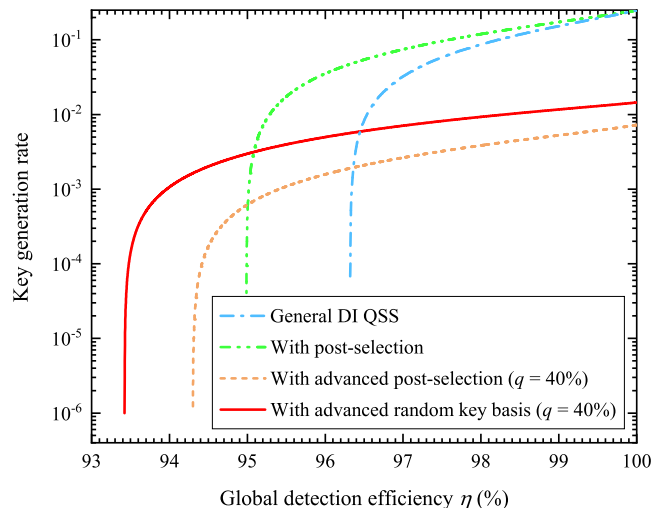


FIG. 5: (Color online) The key generation rate of DI QSS in the case of using the four active improvement strategies as a function of the global detection efficiency η with the fidelity $F = 1$.

$\eta_d = 98\%$ and $\eta_c = 99\%$ in our simulations. The DI QSS protocol with the advanced random key generation basis strategy ($q = 20\%$) has the longest photon transmission distance of 0.799 km. This means that the maximal secure communication distance between any two users achieves 1.384 km. If we increase the value of q to 40%, the maximal secure communication distance between any two users can achieve 1.43 km, which is about 5.5 times of the initial value (0.26 km) [42]. Meanwhile, DI QSS with the advanced random key generation basis strategy ($q = 20\%$) has the highest key generation rate when photons are transmitted over long distances. For example, in the case of $L = 0.3$ km, its key generation rate is about 3.5 times of that with the advanced postselection strategy ($q = 20\%$). Based on the comparison results, the DI QSS protocol with advanced random key generation basis strategy has big advantages in practical applications.

VI. DISCUSSION AND CONCLUSION

In the paper, we propose the DI QSS protocol with the advanced random key generation basis, which can effectively improve DI QSS's noise tolerance and maximal secure photon transmission distance. In this work, we analyze DI QSS's conditional entropy bound by simplifying it to the qubit bound, and numerically and analytically evaluate its key generation rate. The advanced random key generation basis strategy can effectively increase Eve's uncertainty about the key generation basis and the measurement results, which eventually improves the protocol's resistance to noise.

Here, we consider the tripartite DI QSS protocol. Actually, we can use the m -party Svetlichny polynomial with the form of CHSH polynomials to extend it to the

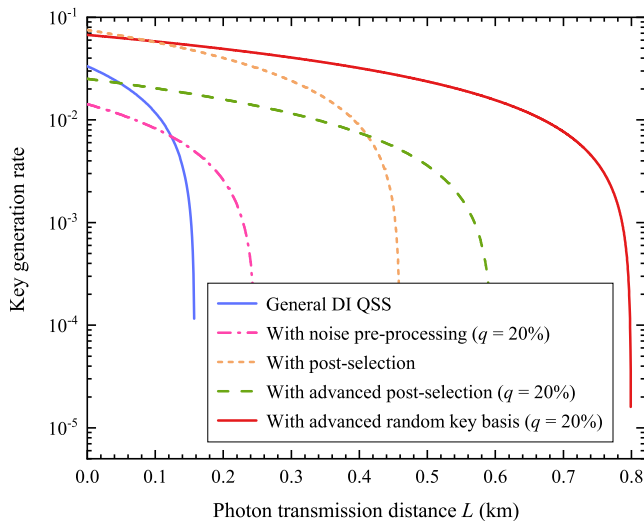


FIG. 6: (Color online) The key generation rate of the DI QSS protocol in five cases as a function of the photon transmission distance L . Here, we control the efficiency $\eta_a = 98\%$, $\eta_c = 99\%$ and the fidelity $F = 1$.

general multipartite DI QSS protocol with advanced random key generation basis strategy [51]. The m -party Svetlichny inequality has the form of

$$S_m = \langle S_{m-1}M_2 \rangle + \langle S'_{m-1}M_1 \rangle \leq 2^{m-1}. \quad (31)$$

We can use the violation of m -party Svetlichny inequality to guarantee the nonlocal correlation among the particles in m users and realize the general m -party DI QSS with advanced random key generation basis strategy.

In our DI QSS protocol, Alice, Bob, and Charlie independently select the measurement basis to measure their photons, which results in the final key generation rate decreasing due to the “sifting” effect (only two of the twelve basis combinations are used to generate keys, the measurement results corresponding to the basis combinations $\{A_1B_1C_2\}$ and $\{A_2B_1C_1\}$ should be discarded). In particular, with the growth of the user or measurement settings number, the “sifting” effect would be more serious. Two possible methods may be applied to avoid this degradation [45]. The first method is to use the quantum memory. In detail, three users receive and store all quantum states in quantum memories. Then, they publicly announce their basis choices and measure their own photon after agreeing on the basis choices (avoiding the case of choosing $\{A_1B_1C_2\}$ and $\{A_2B_1C_1\}$). The second method is the most hopeful one, where Alice, Bob, and Charlie need to share a long enough pre-shared key in advance to coordinate their measurement basis selection during the key generation rounds.

Finally, we discuss the experimental realization of our DI QSS protocol. The DI QSS protocol requires to distribute high-quality GHZ state through quantum channels. The generation of three-photon GHZ states with high fidelity has been extensively studied [66–69]. One

common GHZ state generation method depends on the post selection [66, 68], in which the generated GHZ state is destroyed by the photon detection and cannot be used. In 2014, Hamel *et al.* [67] eliminated the limitation of the outcome post selection by cascading two SPDC sources for directly generating three-photons polarization GHZ states with the fidelity of 86%. Recently, by using the phase-stable source, the fidelity of the target GHZ state was increased to over 96% [69]. Only the phase-flip error may occur in the practical GHZ state generation [67, 69], which will cause the quantum bit error in the key generation process. In this way, the imperfect GHZ state generated in Ref. [69] would cause the QBER of 4%. This QBER is below the noise threshold 9.231%, so that the current GHZ state generation technology in Ref. [69] satisfies the requirement of our DI QSS protocol with advanced random key generation basis strategy. Combining the practical high-efficient SNSPD, our DI QSS protocol with advanced random key generation basis strategy has potential to demonstrate with current experimental technology. On the other hand, the photon transmission loss and decoherence caused by the practical noisy channels severely degrade the entanglement and reduce DI QSS’s secret key generation rate. Since DI QSS has to transmit entanglement photon pairs to multiple users, any photon loss that occurs during transmission can break the entanglement, so it has relatively low resistance to photon loss. Quantum repeater provides a promising way to construct high-quality long-distance entanglement channel [70, 71]. Combining quantum repeater with the DI QSS protocol may further increase the secure communication distance and realize the long-distance DI QSS.

In conclusion, DI QSS can provide the highest security for QSS under practical imperfect experimental conditions. However, DI QSS protocol has quite low noise tolerance threshold and high global detection efficiency requirement, which largely limit its experimental demonstration and application. To reduce DI QSS’s experimental requirements and improve its performance in practical noisy experiment, we propose a new DI QSS protocol with advanced random key generation basis strategy. The advanced random key generation basis strategy combine the random key generation basis, noise preprocessing, and postselection strategies, which can effectively increase the total key secrecy rate to Eve, and thus effectively increase DI QSS’s noise tolerance threshold from 7.147% to 9.231% (29.16% growth) and reduce the global detection efficiency requirement from initial 96.32% to 93.41% ($q \rightarrow 50\%$). In this way, the maximal secure communication distance between any two users can be increased from 0.26 km to 1.43 km (about 5.5 times). Meanwhile, our DI QSS can reuse some discarded items in original DI QSS protocol [42] and reduce the entanglement resource consumption. DI QSS requires to distribute high-quality GHZ state. The requirement for high-quality GHZ state can be satisfied with current GHZ source. Our DI QSS protocol can be extended to the general multipartite condition and has potential to demon-

strate with current experimental technology, which can effectively promote DI QSS's experimental demonstration and applications in the future.

Acknowledgement

This work was supported by the National Natural Science Foundation of China under Grants No. 12175106 and No. 92365110, the Natural Science Foundation of Jiangsu Province of China under Grants No. BK20240611 and No. BK20240612.

Appendix A: Reduce the DI conditional entropy bound of Eve to the qubit bound

In Sec. IV A, we first constrain the conditional entropy of Eve's knowledge about Alice's key with the correlation $\langle \bar{A}_i \otimes B \rangle$. Then, we establish a full DI qubit bound on $\langle \bar{A}_i \otimes B \rangle$. Finally, we perform a convexity analysis of the DI conditional entropy bound [46].

In the DI scenario, we note that all devices are untrusted, so that the measurement basis used by three users may be potentially under Eve's control. As a result, all measurement bases need to be reparametrized in the following analysis. By simplifying the DI conditional entropy bound to the qubit system, the two-basis

(random key generation basis) variant has a conditional entropy bound as

$$\begin{aligned} H(A|E) &= \lambda H(A_1|E) + \bar{\lambda} H(A_2|E) \\ &\geq g\left(\sqrt{\lambda \langle \bar{A}_1 \otimes B \rangle^2 + \bar{\lambda} \langle \bar{A}_2 \otimes B' \rangle^2}\right), \end{aligned} \quad (\text{A.1})$$

where \bar{A}_1 and \bar{A}_2 are the Pauli observations orthogonal to A_1 and A_2 in the X-Y plane of the Bloch sphere, respectively. B and B' are observations with any given eigenvalue ± 1 on Bob's subsystem. In DI-type protocols, we do not directly obtain the correlation between Alice's and Bob's subsystems ($\langle \bar{A}_i \otimes B \rangle$, $i = 1, 2$). We maximally estimate Eve's information about the measurement results of A_1 and A_2 by the correlation operator of Bob's subsystem with the virtual complementary \bar{A}_1 and \bar{A}_2 . Let the lower bound function $g(x) = 1 - h(\frac{1}{2} + \frac{1}{2}x)$.

In terms of $H(A|E)$, in order to find the optimal value of the conditional entropy bound, we need to parameterize all the qubit operators in the X-Y plane of the Bloch sphere. Let the observations $B = \cos \varphi_B \sigma_x + \sin \varphi_B \sigma_y$ and $B' = \cos \varphi'_B \sigma_x + \sin \varphi'_B \sigma_y$. The $g(\sqrt{x})$ function is monotonically increasing and convex in the $x \in [0, 1]$. Therefore, we choose the optimal φ_B and φ'_B by Cauchy-Schwarz inequality to maximize the lower bound of $H(A|E)$ with the form of

$$\begin{aligned} &\lambda \langle \bar{A}_1 \otimes B \rangle^2 + \bar{\lambda} \langle \bar{A}_2 \otimes B' \rangle^2 \\ &= \lambda \langle \bar{A}_1 \otimes (\cos \varphi_B \sigma_x + \sin \varphi_B \sigma_y) \rangle^2 + \bar{\lambda} \langle \bar{A}_2 \otimes (\cos \varphi'_B \sigma_x + \sin \varphi'_B \sigma_y) \rangle^2 \\ &= \lambda (\cos \varphi_B \langle \bar{A}_1 \otimes \sigma_x \rangle + \sin \varphi_B \langle \bar{A}_1 \otimes \sigma_y \rangle)^2 + \bar{\lambda} (\cos \varphi'_B \langle \bar{A}_2 \otimes \sigma_x \rangle + \sin \varphi'_B \langle \bar{A}_2 \otimes \sigma_y \rangle)^2 \\ &\leq \lambda \left[\sqrt{(\cos^2 \varphi_B + \sin^2 \varphi_B) (\langle \bar{A}_1 \otimes \sigma_x \rangle^2 + \langle \bar{A}_1 \otimes \sigma_y \rangle^2)} \right]^2 \\ &\quad + \bar{\lambda} \left[\sqrt{(\cos^2 \varphi'_B + \sin^2 \varphi'_B) (\langle \bar{A}_2 \otimes \sigma_x \rangle^2 + \langle \bar{A}_2 \otimes \sigma_y \rangle^2)} \right]^2 \\ &= \lambda (\langle \bar{A}_1 \otimes \sigma_x \rangle^2 + \langle \bar{A}_1 \otimes \sigma_y \rangle^2) + \bar{\lambda} (\langle \bar{A}_2 \otimes \sigma_x \rangle^2 + \langle \bar{A}_2 \otimes \sigma_y \rangle^2). \end{aligned} \quad (\text{A.2})$$

To maximize Eve's uncertainty about the measurement basis, we first parameterize Alice's measurement bases as

$$\begin{aligned} A_1 &= \cos \frac{\varphi_A}{2} \sigma_x - \sin \frac{\varphi_A}{2} \sigma_y, \\ A_2 &= \cos \frac{\varphi_A}{2} \sigma_x + \sin \frac{\varphi_A}{2} \sigma_y. \end{aligned} \quad (\text{A.3})$$

Their corresponding virtual complementary operators

are

$$\begin{aligned} \bar{A}_1 &= \sin \frac{\varphi_A}{2} \sigma_x + \cos \frac{\varphi_A}{2} \sigma_y, \\ \bar{A}_2 &= -\sin \frac{\varphi_A}{2} \sigma_x + \cos \frac{\varphi_A}{2} \sigma_y. \end{aligned} \quad (\text{A.4})$$

Substituting \bar{A}_1 and \bar{A}_2 into Eq. (A.2) can obtain the objective function of the optimization problem as

$$\begin{aligned}
\lambda \langle \bar{A}_1 \otimes B \rangle^2 + \bar{\lambda} \langle \bar{A}_2 \otimes B' \rangle^2 &\leq \lambda \left(\langle \bar{A}_1 \otimes \sigma_x \rangle^2 + \langle \bar{A}_1 \otimes \sigma_y \rangle^2 \right) + \bar{\lambda} \left(\langle \bar{A}_2 \otimes \sigma_x \rangle^2 + \langle \bar{A}_2 \otimes \sigma_y \rangle^2 \right) \\
&= \lambda \left[\left\langle \left(\sin \frac{\varphi_A}{2} \sigma_x + \cos \frac{\varphi_A}{2} \sigma_y \right) \otimes \sigma_x \right\rangle^2 + \left\langle \left(\sin \frac{\varphi_A}{2} \sigma_x + \cos \frac{\varphi_A}{2} \sigma_y \right) \otimes \sigma_y \right\rangle^2 \right] \\
&+ \bar{\lambda} \left[\left\langle \left(-\sin \frac{\varphi_A}{2} \sigma_x + \cos \frac{\varphi_A}{2} \sigma_y \right) \otimes \sigma_x \right\rangle^2 + \left\langle \left(-\sin \frac{\varphi_A}{2} \sigma_x + \cos \frac{\varphi_A}{2} \sigma_y \right) \otimes \sigma_y \right\rangle^2 \right] \\
&= \sin^2 \frac{\varphi_A}{2} (E_{XX}^2 + E_{XY}^2) + \cos^2 \frac{\varphi_A}{2} (E_{YX}^2 + E_{YY}^2) \\
&+ 2(2\lambda - 1) \sin \frac{\varphi_A}{2} \cos \frac{\varphi_A}{2} (E_{XX} E_{YX} + E_{XY} E_{YY}), \tag{A.5}
\end{aligned}$$

where Pauli operators $E_{XX} = \langle \sigma_x \otimes \sigma_x \rangle$, $E_{YX} = \langle \sigma_y \otimes \sigma_x \rangle$, $E_{XY} = \langle \sigma_x \otimes \sigma_y \rangle$, and $E_{YY} = \langle \sigma_y \otimes \sigma_y \rangle$.

Now, we need to find constraints on the optimization problem (A.5) in terms of the nonlocal correlations S and the Pauli operators (E_{XX} , E_{YX} , E_{XY} , and E_{YY}) to further bound (A.1).

Firstly, in terms of DI QSS, we emphasize that the

tripartite nonlocal correlation is embodied in the CHSH expectation values S between Alice and Bob in Sec. II B. In imperfect measurements, maximizing the CHSH expectation value S between Alice and Bob can increase the key secrecy rate to Eve. For the first case of the CHSH polynomial S between Alice and Bob ($S = S_{AB}$), we rewrite S_{AB} in Eq. (7) into qubit operator form

$$\begin{aligned}
S_{AB} &= \langle A_1 \otimes B_2 \rangle + \langle A_2 \otimes B_2 \rangle + \langle A_1 \otimes B_3 \rangle - \langle A_2 \otimes B_3 \rangle \\
&= \langle (A_1 + A_2) \otimes B_2 \rangle + \langle (A_1 - A_2) \otimes B_3 \rangle \\
&= 2 \cos \frac{\varphi_A}{2} \langle \sigma_x \otimes B_2 \rangle - 2 \sin \frac{\varphi_A}{2} \langle \sigma_y \otimes B_3 \rangle. \tag{A.6}
\end{aligned}$$

We use B_2 and B_3 to maximize Eq. (A.6) by the

Cauchy-Schwarz inequality as

$$\begin{aligned}
\frac{S_{AB}}{2} &= \cos \frac{\varphi_A}{2} \langle \sigma_x \otimes B_2 \rangle - \sin \frac{\varphi_A}{2} \langle \sigma_y \otimes B_3 \rangle \\
&= \cos \frac{\varphi_A}{2} (\cos \varphi_{B_2} \langle \sigma_x \otimes \sigma_x \rangle + \sin \varphi_{B_2} \langle \sigma_x \otimes \sigma_y \rangle) \\
&- \sin \frac{\varphi_A}{2} (\cos \varphi_{B_3} \langle \sigma_y \otimes \sigma_x \rangle + \sin \varphi_{B_3} \langle \sigma_y \otimes \sigma_y \rangle) \\
&\leq \cos \frac{\varphi_A}{2} \sqrt{\langle \sigma_x \otimes \sigma_x \rangle^2 + \langle \sigma_x \otimes \sigma_y \rangle^2} - \sin \frac{\varphi_A}{2} \sqrt{\langle \sigma_y \otimes \sigma_x \rangle^2 + \langle \sigma_y \otimes \sigma_y \rangle^2} \\
&= \cos \frac{\varphi_A}{2} \sqrt{E_{XX}^2 + E_{XY}^2} - \sin \frac{\varphi_A}{2} \sqrt{E_{YX}^2 + E_{YY}^2}. \tag{A.7}
\end{aligned}$$

Similarly, for the second case of the CHSH polynomial S between Alice and Bob ($S = S'_{AB}$), we rewrite S'_{AB} in

Eq. (7) with the form of qubit operator as

$$\begin{aligned}
S'_{AB} &= \langle A_2 \otimes B_3 \rangle + \langle A_2 \otimes B_2 \rangle + \langle A_1 \otimes B_3 \rangle - \langle A_1 \otimes B_2 \rangle \\
&= \langle (A_1 + A_2) \otimes B_3 \rangle - \langle (A_1 - A_2) \otimes B_2 \rangle \\
&= 2 \cos \frac{\varphi_A}{2} \langle \sigma_x \otimes B_3 \rangle + 2 \sin \frac{\varphi_A}{2} \langle \sigma_y \otimes B_2 \rangle. \tag{A.8}
\end{aligned}$$

We use B_2 and B_3 to maximize Eq. (A.8) by the Cauchy-Schwarz inequality as

$$\begin{aligned}
\frac{S'_{AB}}{2} &= \cos \frac{\varphi_A}{2} \langle \sigma_x \otimes B_3 \rangle + \sin \frac{\varphi_A}{2} \langle \sigma_y \otimes B_2 \rangle \\
&= \cos \frac{\varphi_A}{2} (\cos \varphi_{B_3} \langle \sigma_x \otimes \sigma_x \rangle + \sin \varphi_{B_3} \langle \sigma_x \otimes \sigma_y \rangle) \\
&\quad + \sin \frac{\varphi_A}{2} (\cos \varphi_{B_2} \langle \sigma_y \otimes \sigma_x \rangle + \sin \varphi_{B_2} \langle \sigma_y \otimes \sigma_y \rangle) \\
&\leq \cos \frac{\varphi_A}{2} \sqrt{\langle \sigma_x \otimes \sigma_x \rangle^2 + \langle \sigma_x \otimes \sigma_y \rangle^2} + \sin \frac{\varphi_A}{2} \sqrt{\langle \sigma_y \otimes \sigma_x \rangle^2 + \langle \sigma_y \otimes \sigma_y \rangle^2} \\
&= \cos \frac{\varphi_A}{2} \sqrt{E_{XX}^2 + E_{XY}^2} + \sin \frac{\varphi_A}{2} \sqrt{E_{YX}^2 + E_{YY}^2}. \tag{A.9}
\end{aligned}$$

In conclusion, based on Eq. (8) and the absolute value inequality $|a \pm b| \leq |a| + |b|$, we have

$$\begin{aligned}
\frac{S}{2} &\leq \left| \cos \frac{\varphi_A}{2} \right| \sqrt{E_{XX}^2 + E_{XY}^2} \\
&\quad + \left| \sin \frac{\varphi_A}{2} \right| \sqrt{E_{YX}^2 + E_{YY}^2}. \tag{A.10}
\end{aligned}$$

Then, we bound E_{XX} , E_{YX} , E_{XY} , E_{YY} . For arbitrary normalized Bloch vectors $\mathbf{a} = (a_x \ a_y)$ and $\mathbf{b} = (b_x \ b_y)$ in the X-Y plane, the linear combinations $\mathbf{a} \cdot \boldsymbol{\sigma}$ and $\mathbf{b} \cdot \boldsymbol{\sigma}$ have eigenvalues ± 1 , where $\boldsymbol{\sigma} = (\sigma_x \ \sigma_y \ \sigma_z)$. Thus, for any measurement operator, we have

$$\begin{aligned}
\langle (\mathbf{a} \cdot \boldsymbol{\sigma}) \otimes (\mathbf{b} \cdot \boldsymbol{\sigma}) \rangle &= \langle (a_x \sigma_x + a_y \sigma_y) \otimes (b_x \sigma_x + b_y \sigma_y) \rangle \\
&= \sum_{m,n} a_m b_n \langle \sigma_m \otimes \sigma_n \rangle \leq 1. \tag{A.11}
\end{aligned}$$

where $m, n \in \{x, y\}$. The right part of Eq. (A.11) can be

given in terms of matrix as

$$\begin{aligned}
&\sum_{m,n} a_m b_n \langle \sigma_m \otimes \sigma_n \rangle \\
&= (a_x \ a_y) \begin{pmatrix} \langle \sigma_x \otimes \sigma_x \rangle & \langle \sigma_x \otimes \sigma_y \rangle \\ \langle \sigma_y \otimes \sigma_x \rangle & \langle \sigma_y \otimes \sigma_y \rangle \end{pmatrix} \begin{pmatrix} b_x \\ b_y \end{pmatrix} \\
&= \mathbf{a}^\top \mathbf{E} \mathbf{b}, \tag{A.12}
\end{aligned}$$

where,

$$\mathbf{E} = \begin{pmatrix} E_{XX} & E_{XY} \\ E_{YX} & E_{YY} \end{pmatrix}. \tag{A.13}$$

Since \mathbf{a} and \mathbf{b} are arbitrary Bloch vectors in the X-Y plane, maximizing Eq. (A.12) by $\mathbf{a} = \mathbf{b}$ yields $\|\mathbf{E}\| \leq 1$, which is equivalent to $\mathbf{E} \mathbf{E}^\top \leq I$. In matrix theory, this means that the matrix

$$I - \mathbf{E} \mathbf{E}^\top = \begin{pmatrix} 1 - E_{XX}^2 - E_{XY}^2 & -E_{XX} E_{YX} - E_{XY} E_{YY} \\ -E_{XX} E_{YX} - E_{XY} E_{YY} & 1 - E_{YX}^2 - E_{YY}^2 \end{pmatrix} \tag{A.14}$$

is semi-positive definite. According to the Sylvester criterion, the matrix is semi-positive definite if and only if

all principal minors of (A.14) are non-negative determinants. We derive the constraints for the matrix as

$$\begin{cases} 1 - E_{XX}^2 - E_{XY}^2 \geq 0, \\ 1 - E_{YX}^2 - E_{YY}^2 \geq 0, \\ (1 - E_{XX}^2 - E_{XY}^2)(1 - E_{YX}^2 - E_{YY}^2) - (E_{XX} E_{YX} + E_{XY} E_{YY})^2 \geq 0. \end{cases} \tag{A.15}$$

To constrain the objective function Eq. (A.5), we de-

note $\lambda \langle \bar{A}_1 \otimes B \rangle^2 + \bar{\lambda} \langle \bar{A}_2 \otimes B' \rangle^2 \geq E_\lambda(S)^2$ and introduce

new variables to simplify the analysis of the maximization problem. Let

$$\begin{aligned} s &= \sin \frac{\varphi_A}{2}, \quad c = \cos \frac{\varphi_A}{2}, \quad \Delta = \cos(\gamma - \mu), \\ E_{XX} &= g \cos \gamma, \quad E_{XY} = g \sin \gamma, \\ E_{YX} &= h \cos \mu, \quad E_{YY} = h \sin \mu. \end{aligned} \quad (\text{A.16})$$

Based on the constraints (A.15), the maximization problem (A.5) is rewritten as

$$\begin{aligned} E_\lambda(S)^2 &= \max \quad s^2 g^2 + c^2 h^2 + 2(2\lambda - 1)scgh\Delta. \\ \text{s.t.} \quad &cg + sh \geq S/2 \\ &g^2 \leq 1 \\ &h^2 \leq 1 \\ &(1 - g^2)(1 - h^2) \geq g^2 h^2 \Delta^2 \\ &c^2 + s^2 = 1 \\ &\Delta^2 \leq 1 \end{aligned} \quad (\text{A.17})$$

Eq. (A.17) can be reduced to a series of semidefinite program problems by using the Lasserre hierarchy [72, 73], which gives the optimal entropy bound in a reasonable time using the MOSEK solver [74]. When $\lambda = \frac{1}{2}$ (i.e., $p = \frac{1}{2}$), Eq. (A.17) degenerates into a quadratic root-finding problem

$$4x(2 - x) + 2(S^2 + 2) + S(x - S)\sqrt{2(1 + x)} = 0. \quad (\text{A.18})$$

In the limit $2 < S \leq 2\sqrt{2}$, we can obtain a strict analytical solution. A reliable solution method for this problem can be found in Ref. [46].

Finally, we obtain DI QSS's conditional entropy bound in (A.1) as

$$H(A|E) \geq g \left(\tilde{E}_\lambda(S) \right), \quad (\text{A.19})$$

where $\tilde{E}_\lambda(S) \equiv \sqrt{\tilde{E}_\lambda(S)^2}$. $\tilde{E}_\lambda(S)^2$ is the maximal value of $E_\lambda(S)^2$ by numerically and analytically solving (A.17).

Appendix B: The white noise model

Decoherence caused by channel noise can severely weaken the nonlocal correlation among users' measurement results. Here, we consider the white noise model, i.e., the target GHZ state may degenerate into eight possible GHZ states with equal probability. Alice, Bob, and Charlie share noisy GHZ states with the form of

$$\rho_{ABC} = F|GHZ\rangle\langle GHZ| + \frac{1-F}{8}I, \quad (\text{B.1})$$

where the fidelity F is the probability that no error occurs in the photon state, and the unit matrix I is composed by the density matrices of the eight possible noisy GHZ states as

$$\begin{aligned} I &= |GHZ_1^+\rangle\langle GHZ_1^+| + |GHZ_1^-\rangle\langle GHZ_1^-| \\ &+ |GHZ_2^+\rangle\langle GHZ_2^+| + |GHZ_2^-\rangle\langle GHZ_2^-| \\ &+ |GHZ_3^+\rangle\langle GHZ_3^+| + |GHZ_3^-\rangle\langle GHZ_3^-| \\ &+ |GHZ_4^+\rangle\langle GHZ_4^+| + |GHZ_4^-\rangle\langle GHZ_4^-|, \end{aligned} \quad (\text{B.2})$$

where

$$\begin{aligned} |GHZ_1^\pm\rangle &= \frac{1}{\sqrt{2}}(|HHH\rangle \pm |VVV\rangle), \\ |GHZ_2^\pm\rangle &= \frac{1}{\sqrt{2}}(|HHV\rangle \pm |VVH\rangle), \\ |GHZ_3^\pm\rangle &= \frac{1}{\sqrt{2}}(|HVH\rangle \pm |VHV\rangle), \\ |GHZ_4^\pm\rangle &= \frac{1}{\sqrt{2}}(|HVV\rangle \pm |VHH\rangle). \end{aligned} \quad (\text{B.3})$$

There are two cases for measuring photons with two key generation basis combinations.

Case 1: Using the first key generation basis combination $\{A_1 B_1 C_1\}$, the measurement results for the eight GHZ states can be written as

$$\begin{aligned} |GHZ_1^+\rangle &= \frac{1}{2}(|+\rangle_a |+\rangle_b |+\rangle_c + |+\rangle_a |-\rangle_b |-\rangle_c + |-\rangle_a |+\rangle_b |-\rangle_c + |-\rangle_a |-\rangle_b |+\rangle_c), \\ |GHZ_2^+\rangle &= \frac{1}{2}(|+\rangle_a |+\rangle_b |+\rangle_c - |+\rangle_a |-\rangle_b |-\rangle_c - |-\rangle_a |+\rangle_b |-\rangle_c + |-\rangle_a |-\rangle_b |+\rangle_c), \\ |GHZ_3^+\rangle &= \frac{1}{2}(|+\rangle_a |+\rangle_b |+\rangle_c - |+\rangle_a |-\rangle_b |-\rangle_c + |-\rangle_a |+\rangle_b |-\rangle_c - |-\rangle_a |-\rangle_b |+\rangle_c), \\ |GHZ_4^+\rangle &= \frac{1}{2}(|+\rangle_a |+\rangle_b |+\rangle_c + |+\rangle_a |-\rangle_b |-\rangle_c - |-\rangle_a |+\rangle_b |-\rangle_c - |-\rangle_a |-\rangle_b |+\rangle_c), \\ |GHZ_1^-\rangle &= \frac{1}{2}(|+\rangle_a |-\rangle_b |+\rangle_c + |-\rangle_a |+\rangle_b |+\rangle_c + |+\rangle_a |+\rangle_b |-\rangle_c + |-\rangle_a |-\rangle_b |-\rangle_c), \\ |GHZ_2^-\rangle &= \frac{1}{2}(|+\rangle_a |-\rangle_b |+\rangle_c + |-\rangle_a |+\rangle_b |+\rangle_c - |+\rangle_a |+\rangle_b |-\rangle_c - |-\rangle_a |-\rangle_b |-\rangle_c), \end{aligned}$$

$$\begin{aligned}
|GHZ_3^-\rangle &= \frac{1}{2}(-|+\rangle_a|-\rangle_b|+\rangle_c + |-\rangle_a|+\rangle_b|+\rangle_c + |+\rangle_a|+\rangle_b|-\rangle_c - |-\rangle_a|-\rangle_b|-\rangle_c), \\
|GHZ_4^-\rangle &= \frac{1}{2}(|+\rangle_a|-\rangle_b|+\rangle_c - |-\rangle_a|+\rangle_b|+\rangle_c + |+\rangle_a|+\rangle_b|-\rangle_c - |-\rangle_a|-\rangle_b|-\rangle_c).
\end{aligned} \tag{B.4}$$

According to the coding rules in Sec. II B: $K_A = K_B \oplus K_C$, when the photon state degenerates to $|GHZ_1^-\rangle$, $|GHZ_2^-\rangle$, $|GHZ_3^-\rangle$, or $|GHZ_4^-\rangle$, three users use the key generation basis combination $\{A_1B_1C_1\}$ to produce the measurement results that would cause players (Bob and Charlie) to obtain the wrong key (*i.e.* bit-flip errors have occurred). Therefore, for the first key generation basis combination $\{A_1B_1C_1\}$, the qubit error rate Q_{111} in the

white noise model is given by

$$Q_{111} = P(a_1b_1c_1 \neq 1) = \frac{1}{8}(1 - F) \times 4 = \frac{1 - F}{2}. \tag{B.5}$$

Case 2: Using the second key generation basis combination $\{A_2B_1C_2\}$, the measurement results for the eight GHZ states can be written as

$$\begin{aligned}
|GHZ_1^+\rangle &= \frac{1}{2}(|+\rangle_a|+\rangle_b|+\rangle_c + |+\rangle_a|-\rangle_b|-\rangle_c + |-\rangle_a|+\rangle_b|-\rangle_c + |-\rangle_a|-\rangle_b|+\rangle_c), \\
|GHZ_2^+\rangle &= \frac{-i}{2}(|+\rangle_a|+\rangle_b|-\rangle_c - |+\rangle_a|-\rangle_b|+\rangle_c - |-\rangle_a|+\rangle_b|+\rangle_c + |-\rangle_a|-\rangle_b|-\rangle_c), \\
|GHZ_3^+\rangle &= \frac{1}{2}(|+\rangle_a|+\rangle_b|+\rangle_c - |+\rangle_a|-\rangle_b|-\rangle_c + |-\rangle_a|+\rangle_b|-\rangle_c - |-\rangle_a|-\rangle_b|+\rangle_c), \\
|GHZ_4^+\rangle &= \frac{-i}{2}(|+\rangle_a|+\rangle_b|-\rangle_c + |+\rangle_a|-\rangle_b|+\rangle_c - |-\rangle_a|+\rangle_b|+\rangle_c - |-\rangle_a|-\rangle_b|+\rangle_c), \\
|GHZ_1^-\rangle &= \frac{1}{2}(|+\rangle_a|+\rangle_b|-\rangle_c + |+\rangle_a|-\rangle_b|+\rangle_c + |-\rangle_a|+\rangle_b|+\rangle_c + |-\rangle_a|-\rangle_b|-\rangle_c), \\
|GHZ_2^-\rangle &= \frac{-i}{2}(-|+\rangle_a|+\rangle_b|+\rangle_c + |+\rangle_a|-\rangle_b|-\rangle_c + |-\rangle_a|+\rangle_b|-\rangle_c - |-\rangle_a|-\rangle_b|+\rangle_c), \\
|GHZ_3^-\rangle &= \frac{1}{2}(|+\rangle_a|+\rangle_b|-\rangle_c - |+\rangle_a|-\rangle_b|+\rangle_c + |-\rangle_a|+\rangle_b|+\rangle_c - |-\rangle_a|-\rangle_b|-\rangle_c), \\
|GHZ_4^-\rangle &= \frac{-i}{2}(|+\rangle_a|+\rangle_b|+\rangle_c + |+\rangle_a|-\rangle_b|-\rangle_c - |-\rangle_a|+\rangle_b|-\rangle_c - |-\rangle_a|-\rangle_b|+\rangle_c).
\end{aligned} \tag{B.6}$$

According to the coding rules in Sec. II B, when the photon state degenerates to $|GHZ_1^+\rangle$, $|GHZ_2^+\rangle$, $|GHZ_3^+\rangle$, or $|GHZ_4^+\rangle$, the measurement results will cause Bob to obtain wrong key. So, for the second key generation basis combination $\{A_2B_1C_2\}$, the QBER Q_{212} in the white noise model is given by

$$Q_{212} = P(a_2b_1c_2 \neq 1) = \frac{1}{8}(1 - F) \times 4 = \frac{1 - F}{2}. \tag{B.7}$$

In conclusion, the measurement results of the two key generation bases have same QBER in the white noise model as

$$Q_1 = Q_{111} = Q_{212} = \frac{1 - F}{2}. \tag{B.8}$$

- [1] M. Hillery, V. Bužek and A. Berthiaume, Quantum secret sharing, *Phys. Rev. A* **59**, 1829 (1999).
- [2] A. Karlsson, M. Koashi and N. Imoto, Quantum entanglement for secret sharing and secret splitting, *Phys. Rev. A* **59**, 162 (1999).
- [3] R. Cleve, D. Gottesman and H.-K. Lo, How to share a quantum secret, *Phys. Rev. Lett.* **83**, 648 (1999).
- [4] L. Xiao, G. L. Long, F. G. Deng and J. W. Pan, Efficient multiparty quantum-secret-sharing schemes,

Phys. Rev. A **69**, 052307 (2004).

- [5] Z. J. Zhang, Y. Li and Z. X. Man, Multiparty quantum secret sharing, *Phys. Rev. A* **71**, 044301 (2005).
- [6] Z. J. Zhang and Z. X. Man, Multiparty quantum secret sharing of classical messages based on entanglement swapping, *Phys. Rev. A* **72**, 022303 (2005).
- [7] D. Markham and B. C. Sanders, Graph states for quantum secret sharing, *Phys. Rev. A* **78**, 042309 (2008).
- [8] A. Tavakoli, I. Herbauts, M. Żukowski and M. Bouren-

- ne, Secret sharing with a single d-level quantum system, *Phys. Rev. A* **92**, 030302 (2015).
- [9] W. P. Grice and B. Qi, Quantum secret sharing using weak coherent states, *Phys. Rev. A* **100**, 022339 (2019).
- [10] B. P. Williams, J. M. Lukens, N. A. Peters, B. Qi and W. P. Grice, Quantum secret sharing with polarization-entangled photon pairs, *Phys. Rev. A* **99**, 062311 (2019).
- [11] Y. Fu, H. L. Yin, T. Y. Chen and Z. B. Chen, Long-distance measurement-device-independent multiparty quantum communication, *Phys. Rev. Lett.* **114**, 090501 (2015).
- [12] Z. K. Gao, T. Li and Z. H. Li, Deterministic measurement-device-independent quantum secret sharing, *Sci. China: Phys. Mech. Astron.* **63**, 120311 (2020).
- [13] X. X. Ju, W. Zhong, Y. B. Sheng and L. Zhou, Measurement-device-independent quantum secret sharing with hyper-encoding, *Chin. Phys. B* **31**, 100302 (2022).
- [14] J. Gu, X. Y. Cao, H. L. Yin and Z. B. Chen, Differential phase shift quantum secret sharing using a twin field, *Opt. Express* **29**, 9165 (2021).
- [15] J. Gu, Y. M. Xie, W. B. Liu, Y. Fu, H. L. Yin and Z. B. Chen, Secure quantum secret sharing without signal disturbance monitoring, *Opt. Express* **29**, 32244 (2021).
- [16] Y. Ouyang, K. Goswami, J. Romero, B. C. Sanders, M.-H. Hsieh and M. Tomamichel, Approximate reconstructability of quantum states and noisy quantum secret sharing schemes, *Phys. Rev. A* **108**, 012425 (2023).
- [17] Y. A. Chen, A. N. Zhang, Z. Zhao, X. Q. Zhou, C. Y. Lu, C. Z. Peng, T. Yang and J. W. Pan, Experimental quantum secret sharing and third-man quantum cryptography, *Phys. Rev. Lett.* **95**, 200502 (2005).
- [18] S. Gaertner, C. Kurtsiefer, M. Bourennane and H. Weinfurter, Experimental demonstration of four-party quantum secret sharing, *Phys. Rev. Lett.* **98**, 020503 (2007).
- [19] H. Lu, Z. Zhang, L. K. Chen, Z. D. Li, C. Liu, L. Li, N. L. Liu, X. F. Ma, Y. A. Chen and J. W. Pan, Secret sharing of a quantum state, *Phys. Rev. Lett.* **117**, 030501 (2016).
- [20] Y. Y. Zhou, J. Yu, Z. H. Yan, X. J. Jia, J. Zhang, C. D. Xie and K. C. Peng, Quantum secret sharing among four players using multipartite bound entanglement of an optical field, *Phys. Rev. Lett.* **121**, 150502 (2018).
- [21] C. Schmid, P. Trojek, M. Bourennane, C. Kurtsiefer, M. Żukowski and H. Weinfurter, Experimental single qubit quantum secret sharing, *Phys. Rev. Lett.* **95**, 230505 (2005).
- [22] B. A. Bell, D. Markham, D. A. Herrera-Martí, A. Marin, W. J. Wadsworth, J. G. Rarity and M. S. Tame, Experimental demonstration of graph-state quantum secret sharing, *Nat. Commun.* **5**, 5480 (2014).
- [23] Y. Cai, J. Roslund, G. Ferrini, F. Arzani, X. Xu, C. Fabre and N. Treps, Multimode entanglement in reconfigurable graph states using optical frequency combs, *Nat. Commun.* **8**, 15645 (2017).
- [24] A. Shen, X. Y. Cao, Y. Wang, Y. Fu, J. Gu, W. B. Liu, C. X. Weng, H. L. Yin and Z. B. Chen, Experimental quantum secret sharing based on phase encoding of coherent states, *Sci. China: Phys. Mech. Astron.* **66**, 143 (2023).
- [25] D. Mayers, Unconditional security in quantum cryptography, *J. ACM* **48**, 351 (2001).
- [26] P. W. Shor and J. Preskill, Simple proof of security of the BB84 quantum key distribution protocol, *Phys. Rev. Lett.* **85**, 441 (2000).
- [27] G. Brassard, N. Lütkenhaus, T. Mor and B. C. Sanders, Limitations on practical quantum cryptography, *Phys. Rev. Lett.* **85**, 1330 (2000).
- [28] J. S. Bell, On the Einstein Podolsky Rosen paradox, *Phys. Phys. Fizika* **1**, 195 (1964).
- [29] Y. Liu, Q. Zhao, M. H. Li, J. Y. Guan, Y. B. Zhang, B. Bai, W. J. Zhang, W. Z. Liu, C. Wu and X. Yuan, Device-independent quantum random-number generation, *Nature* **562**, 548 (2018).
- [30] M. H. Li, X. J. Zhang, W. Z. Liu, S. R. Zhao, B. Bai, Y. Liu, Q. Zhao, Y. X. Peng, J. Zhang and Y. B. Zhang, Experimental realization of device-independent quantum randomness expansion, *Phys. Rev. Lett.* **126**, 050503 (2021).
- [31] A. Acín, N. Gisin and L. Masanes, From Bell's theorem to secure quantum key distribution, *Phys. Rev. Lett.* **97**, 120405 (2006).
- [32] A. Acín, N. Brunner, N. Gisin, S. Massar, S. Pironio and V. Scarani, Device-independent security of quantum cryptography against collective attacks, *Phys. Rev. Lett.* **98**, 230501 (2007).
- [33] S. Pironio, A. Acín, N. Brunner, N. Gisin, S. Massar and V. Scarani, Device-independent quantum key distribution secure against collective attacks, *New J. Phys.* **11**, 045021 (2009).
- [34] L. Zhou, Y. B. Sheng and G. L. Long, Device-independent quantum secure direct communication against collective attacks, *Sci. Bull.* **65**, 12 (2020).
- [35] L. Zhou and Y. B. Sheng, One-step device-independent quantum secure direct communication, *Sci. China: Phys. Mech. Astron.* **65**, 250311 (2022).
- [36] L. Zhou, B. W. Xu, W. Zhong and Y. B. Sheng, Device-independent quantum secure direct communication with single-photon sources, *Phys. Rev. Appl.* **19**, 014036 (2023).
- [37] D. P. Nadlinger, P. Drmota, B. C. Nichol, G. Araneda, D. Main, R. Srinivas, D. M. Lucas, C. J. Ballance, K. Ivanov and E. Y.-Z. Tan, Experimental quantum key distribution certified by Bell's theorem, *Nature* **607**, 682 (2022).
- [38] W. Zhang, T. van Leent, K. Redeker, R. Garthoff, R. Schwonnek, F. Fertig, S. Eppelt, W. Rosenfeld, V. Scarani and C. C. W. Lim, A device-independent quantum key distribution system for distant users, *Nature* **607**, 687 (2022).
- [39] W. Z. Liu, Y. Z. Zhang, Y. Z. Zhen, M. H. Li, Y. Liu, J. Y. Fan, F. H. Xu, Q. Zhang and J. W. Pan, Toward a photonic demonstration of device-independent quantum key distribution, *Phys. Rev. Lett.* **129**, 050502 (2022).
- [40] S. Roy and S. Mukhopadhyay, Device-independent quantum secret sharing in arbitrary even dimensions, *Phys. Rev. A* **100**, 012319 (2019).
- [41] M. G. M. Moreno, S. Brito, R. V. Nery and R. Chaves, Device-independent secret sharing and a stronger form of Bell nonlocality, *Phys. Rev. A* **101**, 052339 (2020).
- [42] Q. Zhang, W. Zhong, M. M. Du, S. T. Shen, X. Y. Li, A. L. Zhang, L. Zhou and Y. B. Sheng, Device-independent quantum secret sharing with noise preprocessing and postselection, *Phys. Rev. A* **110**, 042403 (2024).
- [43] M. Ho, P. Sekatski, E. Y.-Z. Tan, R. Renner, J.-D. Bancal and N. Sangouard, Noisy preprocessing facilitates a photonic realization of device-independent quantum key distribution, *Phys. Rev. Lett.* **124**, 230502 (2020).

- [44] E. Woodhead, A. Acín and S. Pironio, Device-independent quantum key distribution with asymmetric CHSH inequalities, *Quantum* **5**, 443 (2021).
- [45] P. Sekatski, J.-D. Bancal, X. Valcarce, E. Y.-Z. Tan, R. Renner and N. Sangouard, Device-independent quantum key distribution from generalized CHSH inequalities, *Quantum* **5**, 444 (2021).
- [46] M. Masini, S. Pironio and E. Woodhead, Simple and practical DIQKD security analysis via BB84-type uncertainty relations and Pauli correlation constraints, *Quantum* **6**, 843 (2022).
- [47] F. H. Xu, Y. Z. Zhang, Q. Zhang and J. W. Pan, Device-independent quantum key distribution with random postselection, *Phys. Rev. Lett.* **128**, 110506 (2022).
- [48] R. Schwonnek, K. T. Goh, I. W. Primaatmaja, E. Y.-Z. Tan, R. Wolf, V. Scarani and C. C. W. Lim, Device-independent quantum key distribution with random key basis, *Nat. Commun.* **12**, 2880 (2021).
- [49] E. Y.-Z. Tan, C. C.-W. Lim and R. Renner, Advantage distillation for device-independent quantum key distribution, *Phys. Rev. Lett.* **124**, 020502 (2020).
- [50] G. Svetlichny, Distinguishing three-body from two-body nonseparability by a Bell-type inequality, *Phys. Rev. D* **35**, 3066 (1987).
- [51] J. D. Bancal, N. Brunner, N. Gisin and Y. C. Liang, Detecting genuine multipartite quantum nonlocality: a simple approach and generalization to arbitrary dimensions, *Phys. Rev. Lett.* **106**, 020405 (2011).
- [52] L. Masanes, S. Pironio and A. Acín, Secure device-independent quantum key distribution with causally independent measurement devices, *Nat. Commun.* **2**, 238 (2011).
- [53] C. C. W. Lim, C. Portmann, M. Tomamichel, R. Renner and N. Gisin, Device-independent quantum key distribution with local Bell test, *Phys. Rev. X* **3**, 031006 (2013).
- [54] U. Vazirani and T. Vidick, Fully device-independent quantum key distribution, *Phys. Rev. Lett.* **113**, 140501 (2014).
- [55] I. Devetak and A. Winter, Distillation of secret key and entanglement from quantum states, *Proc. R. Soc. A* **461**, 207 (2005).
- [56] R. Augusiak and P. Horodecki, Multipartite secret key distillation and bound entanglement, *Phys. Rev. A* **80**, 042307 (2009).
- [57] S. L. Braunstein and S. Pirandola, Side-channel-free quantum key distribution, *Phys. Rev. Lett.* **108**, 130502 (2012).
- [58] S. Das, S. Bäuml, M. Winczewski and K. Horodecki, Universal limitations on quantum key distribution over a network, *Phys. Rev. X* **11**, 041016 (2021).
- [59] R. Qi, H. Zhang, J. Gao, L. Yin and G.-L. Long, Loophole-free plug-and-play quantum key distribution, *New J. Phys.* **23**, 063058 (2021).
- [60] H.-Y. Su, A simple relation of guessing probability in quantum key distribution, *New J. Phys.* **24**, 093016 (2022).
- [61] H. Wang, D. Liao, D. Guo, J. Xin and J. Kong, Continuous-variable (3, 3)-threshold quantum secret sharing based on one-sided device-independent security, *Phys. Lett. A* **462**, 128650 (2023).
- [62] Y.-Z. Zhen, Y. Mao, Y.-Z. Zhang, F. Xu and B. C. Sanders, Device-independent quantum key distribution based on the Mermin-Peres magic square game, *Phys. Rev. Lett.* **131**, 080801 (2023).
- [63] J. R. Gonzales-Ureta, A. Predojević and A. Cabello, Device-independent quantum key distribution based on Bell inequalities with more than two inputs and two outputs, *Phys. Rev. A* **103**, 052436 (2021).
- [64] D. V. Reddy, R. R. Nerem, S. W. Nam, R. P. Mirin and V. B. Verma, Superconducting nanowire single-photon detectors with 98% system detection efficiency at 1550 nm, *Optica* **7**, 1649 (2020).
- [65] E. Y.-Z. Tan, P. Sekatski, J.-D. Bancal, R. Schwonnek, R. Renner, N. Sangouard and C. C. W. Lim, Improved DIQKD protocols with finite-size analysis, *Quantum* **6**, 880 (2022).
- [66] Y. F. Huang, B. H. Liu, L. Peng, Y. H. Li, L. Li, C. F. Li and G. C. Guo, Experimental generation of an eight-photon Greenberger–Horne–Zeilinger state, *Nat. Commun.* **2**, 546 (2011).
- [67] D. R. Hamel, L. K. Shalm, H. Hübel, A. J. Miller, F. Marsili, V. B. Verma, R. P. Mirin, S. W. Nam, K. J. Resch and T. Jennewein, Direct generation of three-photon polarization entanglement, *Nat. Photonics* **8**, 801 (2014).
- [68] S. Kumar, D. Bhatti, A. E. Jones and S. Barz, Experimental entanglement generation using multiphot beam splitters, *New J. Phys.* **25**, 063027 (2023).
- [69] Z. M. Chaisson, P. F. Poitras, M. Richard, Y. Castonguay-Page, P.-H. Glinel, V. Landry and D. R. Hamel, Phase-stable source of high-quality three-photon polarization entanglement by cascaded down-conversion, *Phys. Rev. A* **105**, 063705 (2022).
- [70] W. J. Munro, K. Azuma, K. Tamaki and K. Nemoto, Inside quantum repeaters, *IEEE J. Sel. Top. Quantum Electron.* **21**, 6400813 (2015).
- [71] J. Dias, M. S. Winnel, W. J. Munro, T. C. Ralph and K. Nemoto, Distributing entanglement in first-generation discrete- and continuous-variable quantum repeaters, *Phys. Rev. A* **106**, 052604 (2022).
- [72] J. B. Lasserre, Global optimization with polynomials and the problem of moments, *SIAM J. Optim.* **11**, 796 (2001).
- [73] D. Henrion and J. B. Lasserre, Convergent relaxations of polynomial matrix inequalities and static output feedback, *IEEE Trans. Autom. Control* **51**, 192 (2006).
- [74] MOSEK solver: https://docs.mosek.com/latest/pythoapi/intro_info.h